



Cite this: *Dalton Trans.*, 2023, **52**, 15313


Received 14th March 2023,

Accepted 21st April 2023

DOI: 10.1039/d3dt00768e

rsc.li/dalton

## High $\text{Mg}^{2+}$ conduction in three-dimensional pores of a metal–organic framework under organic vapors†

Kouhei Aoki,<sup>a</sup> Kenichi Kato<sup>b</sup> and Masaaki Sadakiyo  <sup>\*a</sup>

**We report on high  $\text{Mg}^{2+}$  conduction in a metal–organic framework (MOF), UiO-66, under organic vapors. We prepared a  $\text{Mg}^{2+}$ -containing MOF,  $\text{UiO-66} \supset \{\text{Mg}(\text{TFSI})_2\}_{1.0}$  ( $\text{TFSI}^- = \text{bis}(\text{trifluoromethanesulfonyl})\text{imide}$ ), including  $\text{Mg}^{2+}$  carriers in three-dimensional pores. The compound showed a superionic conductivity above  $10^{-4} \text{ S cm}^{-1}$  under MeCN and MeOH vapors.**

Development of solid-state ionic conductors is one of the current topics in materials chemistry because of their important applications in energy storage or energy producing devices, such as secondary batteries and fuel cells.<sup>1,2</sup> In particular, a good magnesium ion ( $\text{Mg}^{2+}$ ) conductor is required for realization of a solid-state  $\text{Mg}^{2+}$  secondary battery as a rare-element-free energy storage device, while the efficient  $\text{Mg}^{2+}$  conduction in a solid tends to be difficult compared to monovalent ions due to strong electrostatic interactions with neighboring ions.<sup>3</sup>

On another front, metal–organic frameworks (MOFs) have recently attracted much attention due to their designable porous structure which is fundamentally suitable for constructing efficient ion-conducting pathways and introducing ionic carriers. In contrast to many studies on MOFs conducting monovalent ions, such as protons, hydroxide ions, and lithium ions,<sup>4–8</sup> there are few reports on  $\text{Mg}^{2+}$ -conductive MOFs.<sup>9–11</sup> We have focused on creating novel  $\text{Mg}^{2+}$  conductors with porous MOFs. Recently, we reported that the migration of  $\text{Mg}^{2+}$  located in pores can be drastically enhanced by guest vapors because of the formation of highly mobile coordinated carriers.<sup>10,11</sup> Since the ion-conducting pathways are constructed in the pores, the vapor-induced super  $\text{Mg}^{2+}$  conduction in MOFs should deeply depend on the structural features of the pores (e.g. size and dimensionality). However, the

number of reports on vapor-induced super  $\text{Mg}^{2+}$  conduction is currently limited and thus the optimal porous structure of the MOFs is still not revealed well.

In this study, we report on vapor-induced  $\text{Mg}^{2+}$  conduction in a MOF,  $\text{UiO-66} \supset \{\text{Mg}(\text{TFSI})_2\}_x$  ( $x = 0\text{--}2.0$ ,  $\text{TFSI}^- = \text{bis}(\text{trifluoromethanesulfonyl})\text{imide}$ , and  $\text{UiO-66} = \text{Zr}_6\text{O}_4(\text{OH})_4(\text{bdc})_6$  ( $\text{H}_2\text{bdc} = 1,4\text{-benzenedicarboxylic acid}$ )). Previously, we observed vapor-induced  $\text{Mg}^{2+}$  conduction in two different MOFs, containing small-sized one dimensional (1-D) pores ( $\sim 11 \text{ \AA}$ ,  $\text{Mg-MOF-74}$ )<sup>10,12</sup> and large-sized 3-D pores ( $\sim 32 \text{ \AA}$ ,  $\text{MIL-101}$ ).<sup>11,13</sup> To extract the important factors for high  $\text{Mg}^{2+}$  conduction under guest vapors, in this study, we employed UiO-66 as a mother framework, which has small-sized 3-D pores ( $\sim 11 \text{ \AA}$ ).<sup>14</sup> The  $\text{Mg}^{2+}$ -containing sample,  $\text{UiO-66} \supset \{\text{Mg}(\text{TFSI})_2\}_{1.0}$ , showed a very high ionic conductivity above  $10^{-4} \text{ S cm}^{-1}$  ( $25^\circ\text{C}$ , under MeOH or MeCN vapor) with a moderate  $\text{Mg}^{2+}$  transport number ( $t_{\text{Mg}^{2+}} = 0.47$ ). A comparison of the conductivity clearly revealed that the vapor-induced ionic conduction in MOFs deeply relates to the size and dimensionality of the pores.

The Mg salt-containing MOFs were prepared by an impregnation method using an ethanol solution of  $\text{Mg}(\text{TFSI})_2$ , according to previous reports (details are described in the ESI†).<sup>10,11</sup> The amount of  $\text{Mg}^{2+}$  introduced in the MOF sample after washing with EtOH, i.e., the value of  $x$  in  $\text{UiO-66} \supset \{\text{Mg}(\text{TFSI})_2\}_x$ , was determined through inductively coupled plasma atomic emission spectroscopy (ICP-AES). The crystal structure and porous character of the prepared samples were characterized with X-ray powder diffraction (XRPD) and  $\text{N}_2$  adsorption isotherm measurements. Note that we used the sample before washing only for XRPD to detect the bulk  $\text{Mg}(\text{TFSI})_2$  generated on the surface of MOF crystals. As shown in Fig. 1, there is no apparent change in the XRPD patterns after the Mg introduction, confirming that the UiO-66 framework remained. The peaks from bulk  $\text{Mg}(\text{TFSI})_2$ , observed in the sample of  $x = 2.0$ , suggested that the pores were fully occupied by  $\text{Mg}(\text{TFSI})_2$  below that content. This result was confirmed more precisely by  $\text{N}_2$  adsorption isotherm measurements at  $77 \text{ K}$  (Fig. 2). The adsorption amount significantly decreased upon increasing

<sup>a</sup>Department of Applied Chemistry, Faculty of Science Division I, Tokyo University of Science, 1-3 Kagurazaka, Shinjuku-ku, Tokyo 162-8601, Japan. E-mail: sadakiyo@rs.tus.ac.jp

<sup>b</sup>RIKEN SPring-8 Center, Sayo-gun, Hyogo 679-5148, Japan

† Electronic supplementary information (ESI) available: Details of synthesis and physical measurements; Nyquist plots; dc polarization curve; list of activation energy; and XRPD patterns. See DOI: <https://doi.org/10.1039/d3dt00768e>

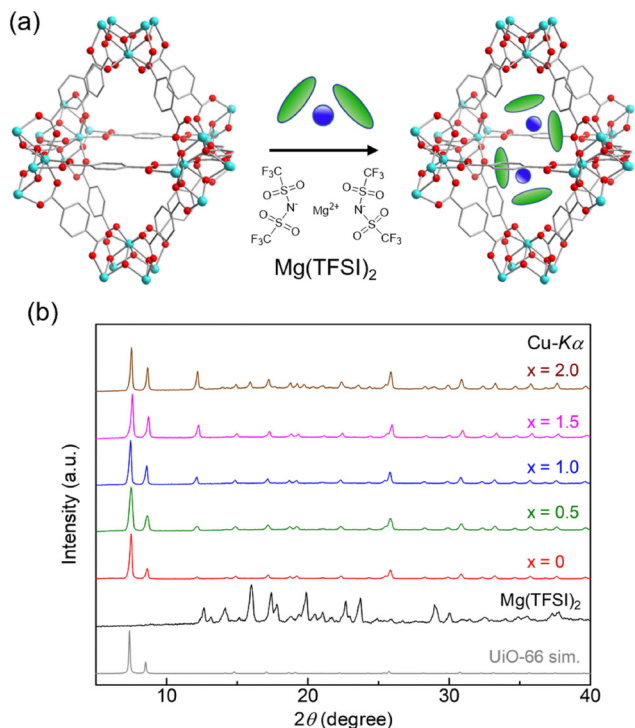


**Fig. 1** (a) Schematic illustration of the introduction of the Mg salts inside the pores of UiO-66. (b) XRPD patterns of bulk  $\text{Mg}(\text{TFSI})_2$  (precisely described as  $[\text{Mg}(\text{H}_2\text{O})_6](\text{TFSI})_2 \cdot 2\text{H}_2\text{O}$ ) and  $\text{UiO-66} \supset \{\text{Mg}(\text{TFSI})_2\}_x$  ( $x = 0-2.0$ ).

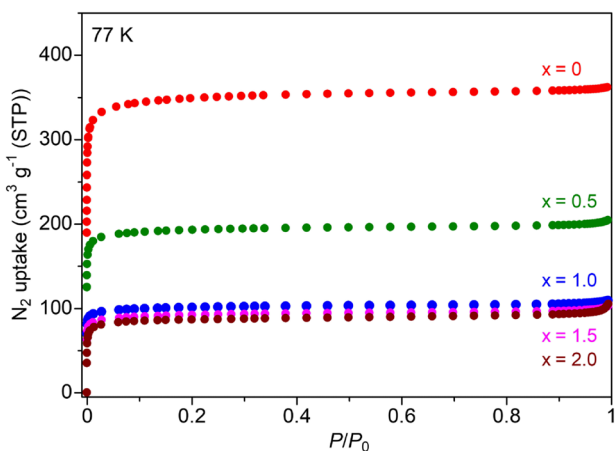


**Fig. 2**  $\text{N}_2$  adsorption isotherms of  $\text{UiO-66} \supset \{\text{Mg}(\text{TFSI})_2\}_x$  ( $x = 0-2.0$ ) at 77 K.

the content of Mg salt below  $x = 1.0$ , while there was almost no change in the higher content ( $x > 1.0$ ). This clearly indicates that the loaded  $\text{Mg}(\text{TFSI})_2$  was introduced inside the pores of UiO-66 and that the pores were fully occupied at  $x = 1.0$ . Note that the remaining  $\text{N}_2$  adsorption after full occupation by the loaded  $\text{Mg}(\text{TFSI})_2$  should be because of some void space produced by the dehydration of the introduced  $\text{Mg}(\text{TFSI})_2$  (precisely described as  $[\text{Mg}(\text{H}_2\text{O})_6](\text{TFSI})_2 \cdot 2\text{H}_2\text{O}$  in air) before

adsorption measurements (*i.e.*, vacuum at 130 °C for a night), which is similar to the case with Mg salt-containing MIL-101.<sup>11</sup>

To study the properties of vapor-induced ionic conduction in this MOF, we performed alternating current (ac) impedance measurements under various organic vapors, such as MeOH, MeCN, EtOH, tetrahydrofuran (THF), diethyl carbonate (DEC), and propylene carbonate (PC), in the same way as our previous reports.<sup>10,11</sup> To avoid the effects of preliminarily included guests such as EtOH and  $\text{H}_2\text{O}$  on ionic conductivity, all the measurements were performed after activation at 130 °C under a dry  $\text{N}_2$  flow for a night (see the ESI†). Fig. 3 summarizes the dependence of the ionic conductivity of the sample  $x = 1.0$  on guest vapors (Nyquist plots are shown in Fig. S1†). The Mg salt-containing UiO-66 sample showed almost no ionic conductivity (below  $10^{-10} \text{ S cm}^{-1}$ ) under dry  $\text{N}_2$  conditions, while a superionic conductivity of above  $10^{-4} \text{ S cm}^{-1}$  was observed under the vapors of small polar guests such as MeOH ( $3.7 \times 10^{-4} \text{ S cm}^{-1}$  at 25 °C) and MeCN ( $2.8 \times 10^{-4} \text{ S cm}^{-1}$  at 25 °C). There is a clear trend that large-sized guest molecules do not lead to high ionic conductivity (*e.g.*, DEC and PC), which is very similar to the cases of previously reported Mg-MOF-74  $\supset \{\text{Mg}(\text{TFSI})_2\}_{0.15}$  and MIL-101  $\supset \{\text{Mg}(\text{TFSI})_2\}_{1.6}$ .<sup>10,11</sup> Note that we also succeeded in determining the transport number of  $\text{Mg}^{2+}$  ( $t_{\text{Mg}^{2+}}$ ) as 0.47 (under MeCN, Fig. S2†), which confirmed that  $\text{UiO-66} \supset \{\text{Mg}(\text{TFSI})_2\}_{1.0}$  is the “ $\text{Mg}^{2+}$ ” conductor and that the value is very similar to the previous cases ( $t_{\text{Mg}^{2+}} = 0.47$  for Mg-MOF-74  $\supset \{\text{Mg}(\text{TFSI})_2\}_{0.15}$  and  $t_{\text{Mg}^{2+}} = 0.41$  for MIL-101  $\supset \{\text{Mg}(\text{TFSI})_2\}_{1.6}$ ).<sup>10,11</sup> The activation energy ( $E_a$ ) of the ionic conduction in the MOF under each guest vapor is listed in Table S1.† The sample of  $x = 1.0$  shows very low activation energy under optimal guest molecules such as MeCN ( $E_a = 0.15 \text{ eV}$ ) and MeOH ( $E_a = 0.18 \text{ eV}$ ), which is also similar to the previous examples of vapor-induced super  $\text{Mg}^{2+}$  conduction in different MOFs ( $E_a = 0.26 \text{ eV}$  for Mg-MOF-74  $\supset \{\text{Mg}(\text{TFSI})_2\}_{0.15}$  under MeOH and  $E_a = 0.18$  for MIL-101  $\supset \{\text{Mg}(\text{TFSI})_2\}_{1.6}$  under MeCN),<sup>10,11</sup> implying a similar trend of the conduction mechanism.

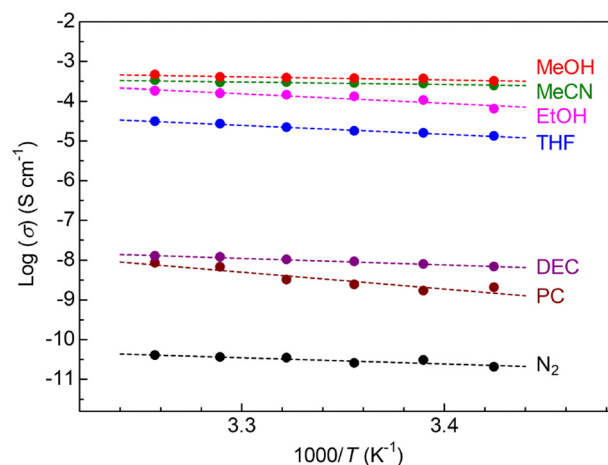


**Fig. 3** Temperature dependence of ionic conductivity of  $\text{UiO-66} \supset \{\text{Mg}(\text{TFSI})_2\}_{1.0}$  under various organic vapors.

To reveal the guest adsorption ability of the sample, we measured adsorption isotherms for the vapors of these small guest molecules, MeOH and MeCN. As shown in Fig. 4, the salt-containing sample ( $x = 1.0$ ) showed a large amount of MeOH adsorption, indicating that the adsorbed guest molecules play a critical role in the high conductivity of this MOF. Note that the XRPD measurements under vacuum and MeOH vapor (Fig. S3†) clearly indicated the inclusion of the adsorbed MeOH molecules inside the MOF; an apparent difference in the intensity ratio of the XRPD patterns before and after exposure to MeOH vapor was observed, while there was almost no change in the lattice constant because of the rigid framework of UiO-66. The difference in the adsorption behavior of the salt-containing MOF compared to the blank MOF ( $x = 0$ ), *i.e.*, the suppressed adsorption amount in a low pressure region and a similar total adsorption amount in a high pressure region, is similar to the case of previously reported MIL-101 and Mg-MOF-74.<sup>10,11</sup> In the case of MeCN, the sample also showed a large amount of adsorption of MeCN (Fig. S4†) and the adsorption behaviour is similar to the case of MeOH. The total amount of MeOH adsorption at high pressure is considerably higher than that of MeCN adsorption in both samples of  $x = 0$  and 1.0. This would be mainly due to the molecular size and a similar tendency was observed in the previous report.<sup>10</sup> The remarkably higher adsorption amount of MeOH in  $x = 0$  would indicate the fact that the mother framework UiO-66 has high affinity for MeOH rather than for MeCN. This would be one of the reasons for the higher conductivity under MeOH rather than under MeCN. Our previous reports revealed that  $\text{Mg}^{2+}$  introduced inside the pores of MOFs can form highly mobile coordinated carriers in the presence of adsorbed guest molecules and thus small guest molecules are advantageous for high ionic conduction.<sup>11</sup> According to the previous literature,<sup>15,16</sup> the coordination geometries of  $\text{Mg}^{2+}$  with MeOH and MeCN are almost the same, *i.e.*, octahedral six-coordination. Considering the fact that a similar ion-conductive behavior under these guests was observed, while

MeOH and MeCN have a remarkable difference in proticity (MeOH:protic and MeCN:aprotic), the vapor-induced increase of ionic conductivity should be caused by a similar mechanism of ionic conduction in this MOF, *i.e.*, the formation of highly mobile  $\text{Mg}^{2+}$  carriers through coordination by the adsorbed guest molecules. The adsorption amounts of both of MeOH and MeCN molecules are enough to form such coordinated carriers ( $>6$  molecules per a formula), which supports this conduction mechanism.

Comparing the ionic conductivity among the  $\text{Mg}^{2+}$ -containing samples with different mother frameworks of UiO-66, MIL-101, and Mg-MOF-74, the order of the conductivity at 25 °C under the optimized conditions is MIL-101 ( $1.9 \times 10^{-3} \text{ S cm}^{-1}$  under MeCN vapor)  $>$  UiO-66 ( $3.7 \times 10^{-4} \text{ S cm}^{-1}$  (MeOH))  $>$  Mg-MOF-74 ( $2.6 \times 10^{-4} \text{ S cm}^{-1}$  (MeOH)). This order is the same as the case under the same small guest molecules (*i.e.*, MeOH and MeCN); for instance, MIL-101 ( $1.9 \times 10^{-3} \text{ S cm}^{-1}$ )  $>$  UiO-66 ( $2.8 \times 10^{-4} \text{ S cm}^{-1}$ )  $>$  Mg-MOF-74 ( $4.6 \times 10^{-5} \text{ S cm}^{-1}$ ) under MeCN. Considering the similar fashion of the ionic conduction under guest vapors in these MOFs as described above, this difference in the conductivity is mainly derived from the difference in the porous structure of the mother frameworks. Since the structural features of the mother frameworks of Mg-MOF-74, MIL-101, and UiO-66 are roughly described as small-sized ( $\sim 11 \text{ \AA}$ ) 1-D pores,<sup>12</sup> large-sized ( $\sim 32 \text{ \AA}$ ) 3-D pores,<sup>13</sup> and small-sized ( $\sim 11 \text{ \AA}$ ) 3-D pores,<sup>14</sup> respectively, we could state that there are two important factors for the vapor-induced ionic conduction in MOFs. First is the pore size; a larger pore size is advantageous for high ionic conductivity (*i.e.*, MIL-101  $>$  UiO-66), which would be because the migration of the large-sized coordinated carriers requires large spacing in the pores. Regarding this point, we think that there is some upper limit of the pore size for the enhancement of the vapor-induced ionic conduction because an extremely large-sized pore (*e.g.*, mesoporous materials) should make the introduced  $\text{Mg}(\text{TFSI})_2$  show the bulk-like physical property. Our previous report revealed that bulk  $\text{Mg}(\text{TFSI})_2$  did not show such vapor-induced ionic conduction as a solid-state compound.<sup>11</sup> Second is the dimensionality of the pores; a higher dimensionality of the pores is advantageous for high ionic conductivity (*i.e.*, UiO-66  $>$  Mg-MOF-74). This would be because the 1-D pores (*i.e.*, 1-D ion-conducting pathway) that locate vertically to the applied electric field prevent the migration of the introduced carriers in the powder sample, while the 3-D pores provide efficient ion-conducting pathways in any direction. Although the vapor-induced super  $\text{Mg}^{2+}$  conduction in MOFs is still under investigation, we could demonstrate that both pore size and dimensionality are some of the most important factors for high  $\text{Mg}^{2+}$  conductivity in MOFs.

## Conclusions

In conclusion, we succeeded in creating a  $\text{Mg}^{2+}$ -conductive MOF, UiO-66  $\supset \{\text{Mg}(\text{TFSI})_2\}_{1.0}$ , showing a superionic conductivity of  $3.7 \times 10^{-4} \text{ S cm}^{-1}$  at 25 °C under the vapor of the

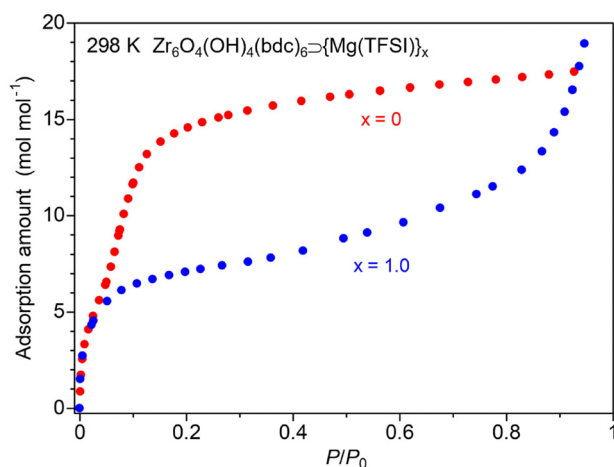


Fig. 4 Adsorption isotherms of blank UiO-66 ( $x = 0$ ) and UiO-66  $\supset \{\text{Mg}(\text{TFSI})_2\}_{1.0}$  ( $x = 1.0$ ) under MeOH vapor.



optimal guest, MeOH. The transport number of  $\text{Mg}^{2+}$  was determined to be  $t_{\text{Mg}^{2+}} = 0.47$ . Conductivity and adsorption measurements revealed that the vapor-induced super  $\text{Mg}^{2+}$  conduction in this MOF would be caused by the formation of the coordinated carriers consisting of introduced  $\text{Mg}^{2+}$  and adsorbed guest molecules. Considering the results of the systematic comparison between the structural features of MOFs and their ionic conductivity, we could state that there are two important factors, *i.e.*, high dimensionality and large pore size, for high ionic conductivity in the vapor-induced  $\text{Mg}^{2+}$  conduction. This should greatly contribute to the development of MOF-based  $\text{Mg}^{2+}$  conductors.

## Conflicts of interest

There are no conflicts to declare.

## Acknowledgements

This work was partly supported by Nippon Sheet Glass Foundation for Materials Science and Engineering, the Shorai Foundation for Science and Technology, The Kurata Grants by The Hitachi Global Foundation, and the Tokuyama Science Foundation, JSPS KAKENHI No. 21K05089, and JST FOREST No. JPMJFR2110. The synchrotron radiation experiments were performed on BL44B2 at SPring-8 with the approval of RIKEN (proposal no. 20200023).

## References

- 1 Y. Kato, S. Hori, T. Saito, K. Suzuki, M. Hirayama, A. Mitsui, M. Yonemura, H. Iba and R. Kanno, High-Power All-Solid-State Batteries Using Sulfide Superionic Conductors, *Nat. Energy*, 2016, **1**, 16030.
- 2 C. Duan, R. J. Kee, H. Zhu, C. Karakaya, T. Chen, S. Ricote, A. Jarry, E. J. Crumlin, D. Hook, R. Braun, N. P. Sullivan and R. O'Hayre, Highly Durable, Coking and Sulfur Tolerant, Fuel-Flexible Protonic Ceramic Fuel Cells, *Nature*, 2018, **557**, 217–222.
- 3 S. Ikeda, M. Takahashi, J. Ishikawa and K. Ito, Solid Electrolytes with Multivalent Cation Conduction. 1. Conducting Species in Mg-Zr-PO<sub>4</sub> system, *Solid State Ionics*, 1987, **23**, 125–129.
- 4 M. Sadakiyo, T. Yamada and H. Kitagawa, Hydrated Proton-Conductive Metal–Organic Frameworks, *ChemPlusChem*, 2016, **81**, 691–701.
- 5 M. Sadakiyo, H. Kasai, K. Kato, M. Takata and M. Yamauchi, Design and Synthesis of Hydroxide Ion-Conductive Metal–Organic Frameworks Based on Salt Inclusion, *J. Am. Chem. Soc.*, 2014, **136**, 1702–1705.
- 6 B. M. Wiers, M.-L. Foo, N. P. Balsara and J. R. Long, A Solid Lithium Electrolyte via Addition of Lithium Isopropoxide to a Metal–Organic Framework with Open Metal Sites, *J. Am. Chem. Soc.*, 2011, **133**, 14522–14525.
- 7 M. Sadakiyo and H. Kitagawa, Ion-Conductive Metal–Organic Frameworks, *Dalton Trans.*, 2021, **50**, 5385–5397.
- 8 K. Nath, A. B. Rahaman, R. Moi, K. Maity and K. Biradha, Porous Li-MOF as a solid-state electrolyte: exploration of lithium ion conductivity through bio-inspired ionic channels, *Chem. Commun.*, 2020, **56**, 14873–14876.
- 9 S. S. Park, Y. Tulchinsky and M. Dincă, Single-Ion Li<sup>+</sup>, Na<sup>+</sup>, and Mg<sup>2+</sup> Solid Electrolytes Supported by a Mesoporous Anionic Cu–Azolate Metal–Organic Framework, *J. Am. Chem. Soc.*, 2017, **139**, 13260–13263.
- 10 Y. Yoshida, K. Kato and M. Sadakiyo, Vapor-Induced Superionic Conduction of Magnesium Ions in a Metal–Organic Framework, *J. Phys. Chem. C*, 2021, **125**, 21124–21130.
- 11 Y. Yoshida, T. Yamada, Y. Jing, T. Toyao, K. Shimizu and M. Sadakiyo, Super  $\text{Mg}^{2+}$  Conductivity around  $10^{-3} \text{ S cm}^{-1}$  Observed in a Porous Metal–Organic Framework, *J. Am. Chem. Soc.*, 2022, **144**, 8669–8675.
- 12 P. D. C. Dietzel, R. Blom and H. Fjellvåg, Base-Induced Formation of Two Magnesium Metal–Organic Framework Compounds with a Bifunctional Tetratopic Ligand, *Eur. J. Inorg. Chem.*, 2008, **23**, 3624–3632.
- 13 G. Férey, C. Mellot-Draznieks, C. Serre, F. Millange, J. Dutour, S. Surblé and I. Margiolaki, A Chromium Terephthalate-Based Solid with Unusually Large Pore Volumes and Surface Area, *Science*, 2005, **309**, 2040–2042.
- 14 J. H. Cavka, S. Jakobsen, U. Olsbye, N. Guillou, C. Lamberti, S. Bordiga and K. P. Lillerud, A New Zirconium Inorganic Building Brick Forming Metal Organic Frameworks with Exceptional Stability, *J. Am. Chem. Soc.*, 2008, **130**, 13850–13851.
- 15 T. Dudev, J. A. Cowan and C. Lim, Competitive Binding in Magnesium Coordination Chemistry: Water versus Ligands of Biological Interest, *J. Am. Chem. Soc.*, 1999, **121**, 7665–7673.
- 16 G. Vyasov, K. Matsumoto and R. Hagiwara, Homoleptic octahedral coordination of  $\text{CH}_3\text{CN}$  to  $\text{Mg}^{2+}$  in the  $\text{Mg}[\text{N}(\text{SO}_2\text{CF}_3)_2]_2\text{--CH}_3\text{CN}$  system, *Dalton Trans.*, 2016, **45**, 2810–2813.

